Laser-induced fluorescence diagnostic via pulsed lasers in an argon plasma

Qiaofeng Zhang, Jinlin Xie, Ming Luo, Xuan Sun, Feibin Fan, Quanming Lu, Weixing Ding, and Yilun Zhu

Citation: Review of Scientific Instruments **89**, 10C119 (2018); doi: 10.1063/1.5038896
View online: https://doi.org/10.1063/1.5038896
View Table of Contents: http://aip.scitation.org/toc/rsi/89/10
Published by the American Institute of Physics

REVIEW OF SCIENTIFIC INSTRUMENTS **89**, 10C119 (2018)

Laser-induced fluorescence diagnostic via pulsed lasers in an argon plasma

Qiaofeng Zhang,[1,2] Jinlin Xie,[1,2,a)] Ming Luo,[1] Xuan Sun,[1,2] Feibin Fan,[2] Quanming Lu,[2] Weixing Ding,[2] and Yilun Zhu[3]
[1]*Department of Engineering and Applied Physics, School of Physical Sciences, University of Science and Technology of China, Hefei 230026, China*
[2]*CAS Key Lab of Geoscience Environment, School of Earth and Space Sciences, University of Science and Technology of China, Hefei 230026, China*
[3]*Department of Electrical and Computer Engineering, University of California, Davis, California 95616, USA*

(Presented 18 April 2018; received 6 May 2018; accepted 7 October 2018; published online 24 October 2018)

Laser-induced fluorescence (LIF) using a pulsed laser is successfully applied in an argon plasma. The laser system consists of a pumping pulse laser fixed at 532 nm and a tunable dye laser. Using a homemade Fabry-Perot interferometer, the large linewidth of the original output is reduced by one order from 4 GHz to 340 MHz. The measured ion temperature is 0.15 eV with a velocity resolution about 200 m/s. It provides great possibility for the combination of LIF and planar LIF using the same pulsed laser system. *Published by AIP Publishing.* https://doi.org/10.1063/1.5038896

I. INTRODUCTION

Laser-induced fluorescence diagnostic (LIF)[1] has been proven to be a powerful tool capable of providing non-intrusive measurements of particle (ions, atoms, radicals, molecules) velocity distributions with high spatial and temporal resolutions in many types of plasma discharges.[2–4] The laser with a narrow linewidth is injected into the plasma to selectively pump the metastable ions with certain speed to the excited state, and then the fluorescence photons are emitted when the excited ions decay back to the ground-state. The fluorescence intensity is proportional to the population of these metastable ions. Via finely scanning the laser wavelength and keeping the laser power output constant, the fluorescence intensity variation as a function of the laser frequency can be measured, which describes the metastable ion populations for different speeds. With a reasonable assumption that the metastable ions are in thermal equilibrium with bulk ions, the ion velocity distribution function (IVDF) is obtained.

Usually lasers with continuous wave (CW) output power around 100 mw are adopted in the LIF scheme[4–7] due to the narrow laser linewidth (around 100 MHz or less) which is helpful to get an IVDF with a fine structure. Compared with the CW laser, the pulsed laser has much strong output and large linewidth. These two characteristics are beneficial to the application of the pulsed laser in Planar LIF[8,9] (PLIF), which is an extension of the LIF technique. The pulsed laser is expanded to a laser sheet to induce fluorescence in a cross section of the plasma, and the fluorescence photons are collected by 2D detector arrays like the CCD chip. The large linewidth of the pulse laser means that the metastable ions are pumped without velocity selection. Then the 2D density profile of metastable ions is acquired.

In this work, a LIF diagnostic system is presented in which the laser system consists of a pumping pulsed laser and a tunable dye laser. The large linewidth 4 GHz of the pulsed laser is reduced to 0.34 GHz using a homemade Fabry-Perot interferometer (FPI) with a parallel plane cavity, which greatly improves the measurement accuracy. The ion temperature in an argon plasma using an oxide-coated cathode is measured by LIF for the first time. Besides the IVDF measurement, the PLIF measurement is also potential to be conducted using the same laser system.

II. EXPERIMENTAL SETUP

An argon plasma column is achieved using a 15-cm-diameter oxide coated cathode biased at −40 V to the grounded grid anode. A static axial magnetic field varying from 180 to 1000 G is generated via 12 sets of magnetic coils to confine the plasma. The plasma source is operated in the pulse mode with 1 Hz repetition frequency and 12 ms pulse length. The typical parameters are working pressure 5×10^{-2} Pa, electron density 5×10^{12} cm^{-3}, and plasma temperature $T_e \approx 10T_i \approx 2$ eV.

A three-level LIF scheme[10] for Ar II is adopted, in which the 611.492 nm (in air) laser pumps the $3d'^2G_{9/2}$ metastable state to the excited state $4p'^2F_{7/2}$. Then the 460.957 nm (in air) fluorescence photons are generated by spontaneous decay from $4p'^2F_{7/2}$ to $4s'^2D_{5/2}$.

The experimental layout is shown in Fig. 1. In configuration A, the laser beam is injected along the axial direction toward the oxide-coated cathode, and the fluorescence signal is measured using a photomultiplier tube (PMT). In configuration B, the laser is injected through one vacuum

---

Note: Paper published as part of the Proceedings of the 22nd Topical Conference on High-Temperature Plasma Diagnostics, San Diego, California, April 2018.

[a)] Author to whom correspondence should be addressed: jlxie@ustc.edu.cn

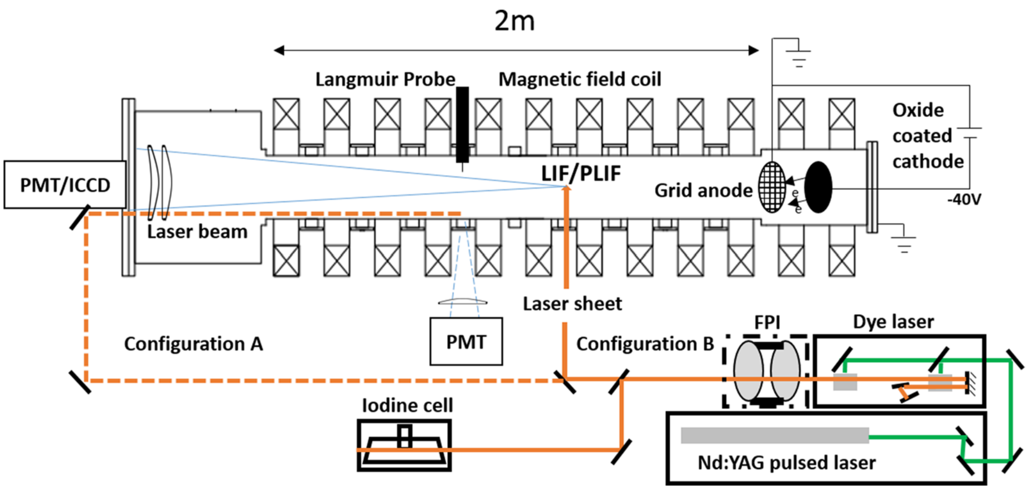

FIG. 1. Device and LIF apparatus.

port in the small cross section of the device and the fluorescence signal is collected via an optics system located at one end of the device. The optics system with large aperture size (18 cm diameter) is composed by a plano-convex lens and a meniscus lens (equivalent focal length 16 cm), which has been optimized to increase the collection solid angle and correct field curvature (for future PLIF application). For both configurations, an interference bandpass filter centered at 460.9 nm with bandwidth 1 nm is applied in front of the fluorescence detector to enhance the S/N ratio.

A 532 nm Nd:YAG laser with 10 ns pulse length and 30 Hz repetition frequency is used to pump a tunable dye laser. Mix Rh B/Rh 101 is chosen as the laser dye due to its high energy conversion efficiency around 615 nm. The maximum output power is around 180 mJ with pump laser power at 700 mJ. The Littrow cavity is used in the dye laser to get a tuning range large than 10 nm. An iodine absorption technique is used to *in situ* monitor the laser wavelength.[6,11]

Since the laser and the plasma source work at different repetition frequencies, the time sequence should be carefully arranged. A 1 Hz transistor-transistor logic (TTL) signal acts as the main triggger signal, which simultaneously trigs the plasma source and a frequency conversion generator (1 Hz–30 Hz). Then the 30 Hz signal is inputted to a SR645 digital delay generator that provides trigger signals for the laser lamp and Q-switch with an accurate tunable delay, as shown in Fig. 2. Thus the short laser pulse can be injected into the plasma at any preset time during one discharge shot.

In order to obtain the original linewidth of the pulsed laser system, a traditional Fabry-Perot Interferometer (FPI) is applied to measure the laser linewidth.[12] A small fraction (~5%) of the dye laser output is imported to a commercial scanning FPI with Free Spectral Range (FSR) 10 GHz. Via scanning the cavity length, the relationship of the transmission light energy with the cavity length is obtained, which is shown in Fig. 3(a). It is clearly shown that the full width at half maximum (FWHM) of the original laser linewidth is 4 GHz, close to the Doppler broadening width (for 611 nm) of argon ions at 0.5 eV.

FPI is also a natural choice to narrow the laser bandwidth. But the commercial one using a confocal cavity is not suitable for the high power laser due to its limited mode

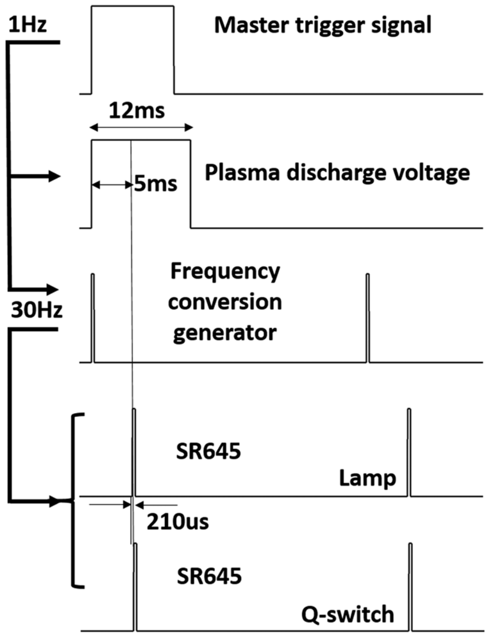

FIG. 2. Timing schematic for the operation of plasma source and laser. The 5 ms delay between the plasma breakdown and the laser can be changed via the SR645. The 210 μs delay is determined by using the pump laser itself.

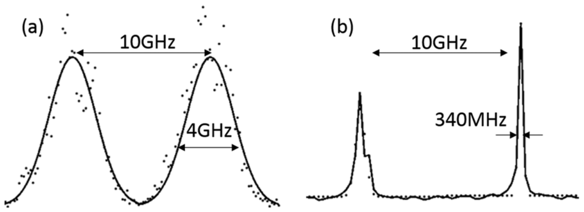

FIG. 3. The linewidth measurement using FPI. The distance between adjacent peaks is 10 GHz determined by the FSR. (a) The original laser and (b) the laser passed through a homemade FPI.

volume. Thus we design a FPI using a parallel plane cavity to realize the linewidth narrowing. The cavity length is around 15 mm. A multilayer piezo ring actuator is adopted to realize a cavity length variation range about 2 μm with positioning accuracy in nm. The reflection of the mirror is 95%, which is a trade-off between the finesse (~60) and the transmitted light energy. The linewidth of the pulse laser passing through this homemade FPI is shown in Fig. 3(b). It is noticed that the laser linewidth has been narrowed from original 4 GHz to 340 MHz, which ensures the fine measurement of IVDF. Experiments via the LIF system with original and narrowed linewidths have been conducted in order to compare the performances.

III. LIF USING ORIGINAL PULSED LASER

The waveforms of the incident laser and the fluorescence signal in one single shot are shown in Fig. 4. The 180 ns delay is consistent with the combination of the cable transit delay 92.5 ns, optical path delay 45 ns, PMT transit time 33 ns, and excited state ion lifetime 8.4 ns. The laser output is set to around 1 mJ to avoid the possible power broadening issue.

The original pulsed laser output is used in the following experiments. The typical LIF experiment with a wavelength adjustment step 0.2 pm is conducted in an argon plasma with magnetic field 180 G and neutral pressure 4×10^{-2} Pa using configuration A. The evolution of the fluorescence intensity is shown in Fig. 5(a). Since the broadening effects such as Zeeman, natural, and pressure are negligible, the measured Full width at half maximum (FWHM) of the LIF signal is dominated by the convolution of the laser linewidth and the real Doppler broadening width. The FWHM of the real Doppler broadening width is estimated as 3 GHz, corresponding to ion temperature 0.2 eV, which is consistent with our previous result.[13] It should be noticed that the collecting optics has a large solid angle and the sampling volume is small in configuration A, which results in a strong LIF signal comparing with the background noise. If the wavelength of the incident laser is absolutely calibrated, the center of the IVDF will be found to red-shift due to the plasma flow velocity along the incident laser direction.

In configuration B, the laser sheet expanded via a cylinder lens is introduced into the cross section, almost the whole plasma cross section is illuminated (~10 cm × 10 cm). The LIF signal is collected via PMT located at the end of the vacuum chamber. The background fluorescence signal that is integrated over the whole plasma column is much stronger than the LIF signal, which is clearly depicted in Fig. 5(b). The plasma is rotating in the azimuthal direction caused by the E × B drift, in which E is the radial electric field. In the whole illumination area, the plasma flow speeds and even the ion temperatures are varied in different radial locations; thus, the FWHM of the LIF signal is greatly broadened. Due to the azimuthal symmetry, the center of the fluorescence distribution is not shifted caused by the plasma rotation.

With the *in situ* iodine absorption method, the two horizontal axes are carefully aligned and the centers of the two distributions are marked as two dashed lines. The frequency gap between them is about 2 GHz, which corresponds to a plasma flow velocity 1400 m/s (0.5 ion sound speed) along the axial direction.

IV. LIF USING PULSED LASER WITH NARROWED LINEWIDTH

The LIF experiments using the pulsed laser with a narrowed linewidth have been performed with configuration A in the similar plasma condition. By synchronously adjusting the center wavelength of the dye laser and the cavity length of homemade FPI, the fine tuning of the final output laser wavelength can be realized with both narrow linewidth and stable power. Since the narrowed linewidth is only 0.34 GHz, the broadening of the fluorescence distribution is fully dominated by the Doppler broadening effect. The measured distribution is shown in Fig. 6, in which the FWHM is 1.8 GHz, corresponding to ion temperature about 0.15 eV. It is also noticed that the velocity resolution is greatly improved to ~200 m/s with this narrowed linewidth.

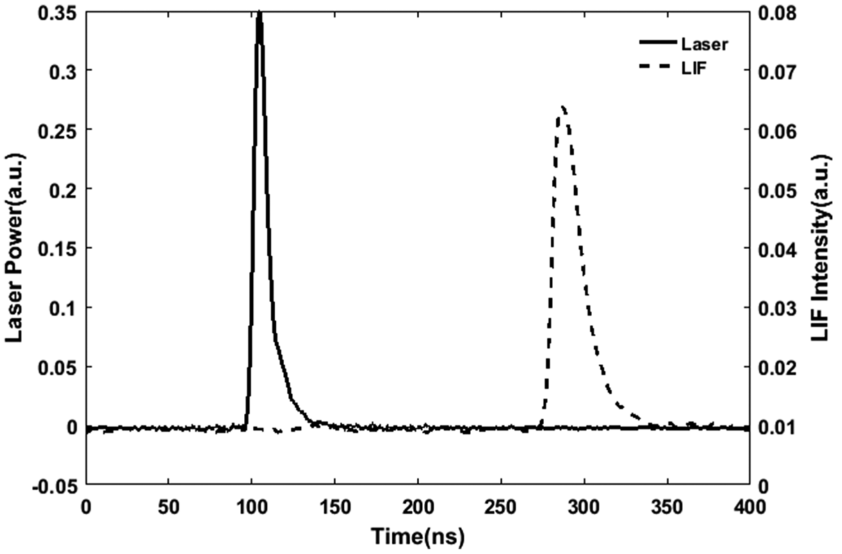

FIG. 4. Timing of the laser pulse and the LIF signal.

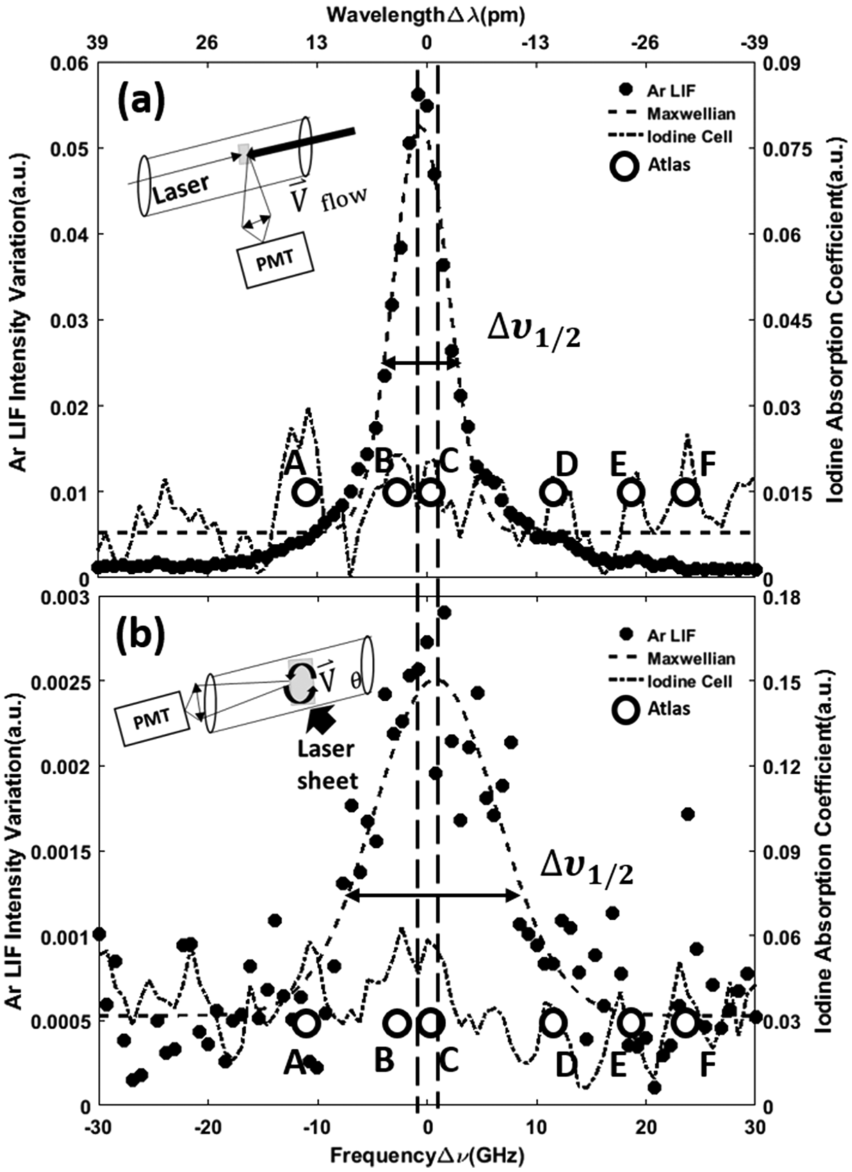

FIG. 5. Original LIF measurements in configurations A and B. The small black dots are the experimental results, which are well fitted using the Maxwellian model marked as the dashed curves. The dotted-dashed line is the *in situ* measured absorption curve of the iodine cell, in which five typical values are marked as hollow circles (A: 611.5003 nm, B: 611.4891 nm, C: 611.4864 nm, D: 611.4735 nm, E: 611.4658, F: 611.4600 nm). The subplots of (a) and (b) are aligned, and the origin of the horizontal coordinate is set at 611.487 nm.

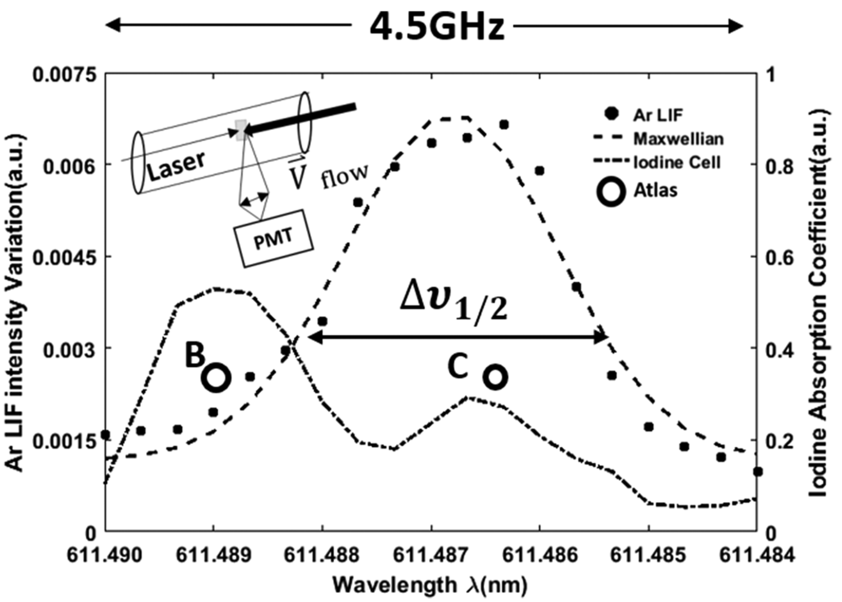

FIG. 6. LIF measurements with narrowed linewidth in configuration A.

V. CONCLUSION

The laser system consisting of a pumping pulse laser and a tunable dye laser has been applied to perform LIF diagnostics in an argon plasma column using an oxide coated cathode. Homemade FPI has been applied to narrow the large linewidth 4 GHz of the original laser output to 0.34 GHz, which ensures the fine measurement of IVDF. The scheme has been successfully applied in an argon plasma using an oxide coated cathode. The ion temperature is measured as 0.15 eV with a high velocity resolution around 200 m/S. It has been demonstrated that the pulsed laser system, with the proper method to narrow the large linewidth, is capable for fine IVDF diagnostic. It also provides a great possibility for the combination of LIF and PLIF diagnostics using the same pulsed laser system, which is an ongoing topic for our group.

ACKNOWLEDGMENTS

This work is supported by the National Nature Science Foundation of China with Contract Nos. 41331067 and 41527804, the Key Research Program of Frontier Sciences CAS (No. QYZDJ-SSW-DQC010), and the National Key Scientific and Research Equipment Development Project of China under Grant No. ZDYZ2013-2.

[1] R. A. Stern and J. A. Johnson III, Phys. Rev. Lett. **34**(25), 1548 (1975).
[2] D. N. Hill, S. Fornaca, and M. G. Wickham, Rev. Sci. Instrum. **54**(3), 309–314 (1983).
[3] D. J. Trevor, N. Sadeghi, T. Nakano *et al.*, Appl. Phys. Lett. **57**(12), 1188–1190 (1990).
[4] X. Jinlin, Y. Zhi, L. Wandong *et al.*, Plasma Sci. Technol. **11**(3), 255 (2009).
[5] G. D. Severn, D. A. Edrich, and R. Mcwilliams, Rev. Sci. Instrum. **69**(1), 10–15 (1998).
[6] A. M. Keesee, E. E. Scime, and R. F. Boivin, Rev. Sci. Instrum. **75**(10), 4091–4093 (2004).
[7] A. K. Hansen, M. Galante, D. McCarren *et al.*, Rev. Sci. Instrum. **81**(10), 10D701 (2010).
[8] B. K. McMillin and M. R. Zachariah, J. Appl. Phys.**77**(11), 5538–5544 (1995).
[9] F. M. Levinton and F. Trintchouk, Rev. Sci. Instrum. **72**(1), 898–905 (2001).
[10] M. J. Goeckner, J. Goree, and T. E. Sheridan, Phys. Fluids B **3**(10), 2913–2921 (1991).
[11] H. J. Woo, K. S. Chung, T. Lho *et al.*, J. Korean Phys. Soc. **48**(2), 260–265 (2006), available at https://escholarship.org/uc/item/1h74s201.
[12] M. G. Littman, Opt. Lett. **3**(4), 138–140 (1978).
[13] G. H. Hu, X. L. Jin, Q. F. Zhang *et al.*, Acta Phys. Sin. **64**(18), 189401 (2015).